

Mycobacterial MazG Is a Novel NTP Pyrophosphohydrolase Involved in Oxidative Stress Response^{*[S]}

Received for publication, December 3, 2009, and in revised form, June 2, 2010. Published, JBC Papers in Press, June 7, 2010, DOI 10.1074/jbc.M109.088872

Liang-dong Lu (吕亮东)^{†§}, Qing Sun (孙青)[§], Xiao-yong Fan (范小勇)[¶], Yi Zhong (钟怡)^{||}, Yu-feng Yao (姚玉峰)^{§1}, and Guo-Ping Zhao (赵国屏)^{†||**††2}

From the [†]State Key Laboratory of Genetic Engineering, Department of Microbiology and Microbial Engineering, School of Life Sciences, Fudan University, Shanghai 200433, China, the [§]Department of Medical Microbiology and Parasitology, Institutes of Medical Sciences, Shanghai Jiao Tong University School of Medicine, Shanghai 200025, China, the [¶]Shanghai Public Health Clinical Center Affiliated with Fudan University, Shanghai 201508, China, the ^{||}Key Laboratory of Synthetic Biology, Institute of Plant Physiology and Ecology, Shanghai Institutes for Biological Sciences, Chinese Academy of Sciences, Shanghai 200032, China, the ^{**}Shanghai-MOST Laboratory of Disease and Health Genomics, Chinese National Human Genome Center at Shanghai, Shanghai 201203, China, and the ^{††}Department of Microbiology and Li Ka Shing Institute of Health Sciences, The Chinese University of Hong Kong, Prince of Wales Hospital, Shatin, New Territories, Hong Kong SAR, China

MazG nucleoside triphosphate pyrophosphohydrolase (NTP-PPase, EC 3.6.1.8) from the avirulent *Mycobacterium tuberculosis* H37Ra contains a spontaneous mutation on a highly conserved residue, resulting in an A219E substitution (MtMazG[A219E]). In this work, we show that mycobacterial MazG from either the virulent *M. tuberculosis* H37Rv (MtMazG) or the fast-growing *Mycobacterium smegmatis* (MsMazG) is a potent NTP-PPase capable of hydrolyzing all canonical (d)NTPs, as well as the mutagenic dUTP and 8-*oxo*-7,8-dihydro-2'-dGTP. However, this hydrolysis activity is diminished by the MtMazG[A219E] mutation. Moreover, deletion of *mazG* in *M. smegmatis* rendered the mycobacteria defective in response to oxidative stress. Importantly, expression of the wild-type MtMazG, but not the A219E mutant, restored cell viability under oxidative stress. Intriguingly, under oxidative stress, both the *mazG*-null and MtMazG[A219E]-expressing *M. smegmatis* strains failed to elevate *relA*, while retaining their ability to up-regulate *sigE*, suggesting a specific role for the MazG NTP-PPase activity in oxidative stress-triggered, transcriptional activation of *relA*. The MtMazG is a homotetramer with each subunit containing a single MazG core domain flanked by two regions, both of which are essential for NTP-PPase activity. Taken together, these results demonstrate that the mycobacterial MazG is a potent NTP-PPase and that this activity is required to maintain the full capacity of the mycobacteria to respond to oxidative stress. Our work implicates a role for the MazG activity in the virulence of *M. tuberculosis*.

Mycobacterium tuberculosis H37Ra is an avirulent relative of the typical laboratory strain H37Rv, both of which are derived

^{*} This work was supported by grants from the National Natural Science Foundation of China (No. 30830002 and No. 30970077), Shanghai Rising-Star Program, Science and Technology Commission of Shanghai Municipality (No. 09QA1403600), the State Key Development Programs for Basic Research of China (973 Program No. 2009CB522605), and the Program for Professor of Special Appointment (Eastern Scholar) at Shanghai Institutions of Higher Learning.

[S] The on-line version of this article (available at <http://www.jbc.org>) contains supplemental Figs. S1–S4 and Tables S1–S3.

¹ To whom correspondence may be addressed. Tel.: 86-21-64671226; Fax: 86-21-64671226; E-mail: yfyao@sjtu.edu.cn.

² To whom correspondence may be addressed. Tel.: 86-21-50801919; Fax: 86-21-50801922; E-mail: gpzhao@sibs.ac.cn.

from the parent strain H37 that was originally isolated from a 19-year-old patient with chronic pulmonary tuberculosis by Edward R. Baldwin in 1905 (1). Our systematic comparison of the complete genomic sequences of H37Rv and H37Ra identified multiple H37Ra-specific single nucleotide polymorphisms (SNPs) affecting about 30 genes including the virulence determinants *phoP*, *nrp*, and *pks12* (2), consistent with the widely accepted notion (3–7) that the virulence attenuation of H37Ra is due to multiple mutations. One of these mutations, the A219E substitution located in a highly conserved sequence of H37Ra MazG, prompted the current study aiming to reveal the function of the corresponding prototype enzyme in *M. tuberculosis* (MtMazG) and compare its role with that of *Escherichia coli* (EcMazG) in adaptation to stress response (8).

The MazG protein belongs to the all- α nucleoside triphosphate pyrophosphohydrolase (NTP-PPase,³ EC 3.6.1.8) superfamily that hydrolyzes *in vitro* all canonical nucleoside triphosphates into monophosphate derivatives and pyrophosphate (PP_i). The physiological substrates of MazG, however, remain elusive (9, 10). Based on the resolved structure of MazG derived from *Sulfolobus solfataricus* and substrate modeling, it is proposed that the MazG family enzymes might perform house-cleaning function by degrading abnormal (d)NTPs, such as dUTP, 2-hydroxy-dATP, and 8-*oxo*-dGTP (9, 10). These modified nucleotides are usually produced under oxidative damage and are mutagenic, *i.e.* their incorporation into genomic DNA causes mispairing and subsequently leads to increased mutation rates. However, to date, this house-cleaning function of MazG remains to be validated experimentally because of the lack of physiological substrates (9, 10).

Accumulating evidence suggests a role for EcMazG in protecting cells from certain toxins. EcMazG regulated programmed cell death by interfering with the function of the MazEF complex, a well characterized toxin-antitoxin (TA) module (8, 11). MazEF was the first identified chromosomal TA module, characterized by the labile antitoxin, MazE, and its

³ The abbreviations used are: NTP-PPase, nucleoside triphosphate pyrophosphohydrolase; PP_i, pyrophosphate; CD, circular dichroism; TA, toxin-antitoxin; 8-*oxo*-dGTP, 8-*oxo*-7,8-dihydro-2'-deoxyguanosine 5'-triphosphate; Mt, *M. tuberculosis*; Ms, *M. smegmatis*; Ec, *E. coli*; WT, wild type.

cognate stable toxin, MazF (12). MazF is an ACA sequence-specific mRNA endoribonuclease that can selectively degrade mRNA via cleavage between the nucleotide residues A and C, thereby inducing a programmed cell death process under stress conditions (13, 14). In *E. coli*, *mazG* is cotranscribed with *mazEF*, while the MazEF proteins inhibit the MazG enzymatic activity both *in vivo* and *in vitro* (8). It was proposed that the EcMazG regulates the MazEF TA module by lowering the cellular (p)ppGpp level, thus protecting the cell from the toxicity of MazF (8). However, it remains to be answered how MazG regulates the cellular (p)ppGpp level and whether such regulation concerns *relA*, which encodes the (p)ppGpp synthetase.

By employing the transposon insertion approaches, previous mouse model studies observed attenuated infection from an H37Rv *mazG* mutant, thereby implicating a role for MtMazG in virulence (15). Despite such advance, however, little is known concerning the enzymatic and physiological functions of MtMazG. In this work, we show that mycobacterial MazG is a potent NTP-PPase capable of hydrolyzing the mutagenic dUTP and 8-*oxo*-dGTP and is required to maintain *Mycobacterium smegmatis* full capacity to respond to oxidative stress, supporting the previously proposed “house cleaning” function of this family protein. However, these functions are diminished in the spontaneous A219E mutant found in H37Ra. Furthermore, mycobacterial *mazG* is an oxidative stress-inducible gene and its NTP-PPase activity is involved in transcriptional activation of *relA* in response to oxidative stress. In contrast to EcMazG, mycobacterial MazG is not involved in starvation response. Unlike mycobacterial MazG, the EcMazG cannot complement for *M. smegmatis mazG* under oxidative stress condition. Taken together, our findings demonstrate that MtMazG is distinct from EcMazG with respect to the properties of enzymes and the possible function in stress response. MtMazG is the first MazG of its kind to be thoroughly characterized, and might be relevant to the virulence of *M. tuberculosis*.

EXPERIMENTAL PROCEDURES

Reagents and Enzyme—Restriction enzymes and *Pfu* DNA polymerase were purchased from Fermentas. T4 DNA ligase, calf-intestinal alkaline phosphatase, and nucleoside triphosphates were obtained from New England Biolabs. The 8-*oxo*-dGTP was purchased from Trilink BioTechnologies, Inc. PiPer pyrophosphate assay kit from Molecular Probes, Inc. was chosen for pyrophosphate detection.

Cloning and Expression of *mazG*—Using the genomic DNA as template, the prototype *mazG* gene from *M. tuberculosis* H37Rv and its mutant type from H37Ra were PCR-amplified with primer TBF22 and TBR22. (All primers used in this study are listed in supplemental Table S1.) The PCR products were digested with NdeI and XhoI and cloned into the corresponding site of pET22b(+) with a fused hexahistidine tag at the C-terminal end of MazG. The resulting vector pET22b-*mazG* was used to transform competent *E. coli* BL21(DE3) cells, which were grown at 37 °C with vigorous shaking to A_{600} of 0.7 in Luria-Bertani (LB) medium containing 100 μ g/ml ampicillin. Expression of MazG was induced with isopropyl-1-thio- β -D-galactopyranoside (0.5 mM) for 12 h at 22 °C. The *mazG* of *E. coli*, *M. smegmatis*, and the truncated variants, including its

site mutants introduced by overlapping PCR, were cloned and expressed in the same way.

Purification of MazG—All operations were carried out at 4 °C. Cells from 200 ml of culture were harvested by centrifugation (7000 \times g, 20 min) and resuspended in 10 ml of binding buffer (20 mM Tris-HCl, pH 7.9, 0.5 M NaCl, 10% glycerol, 10 mM imidazole, 5 mM dithiothreitol). The cells were disrupted by ultrasonication followed by centrifugation at 20,000 \times g for 20 min to remove cell debris and insoluble fraction. The resulting supernatant was applied to a 10-ml column with 1 ml of Ni-Sepharose Fast Flow (GE Healthcare Life Sciences) equilibrated with binding buffer. MazG protein eluted with 100 and 200 mM imidazole was pooled and concentrated by a 30-kDa cutoff ultrafilter (Millipore). The concentrated product was loaded onto Hiload 16/60 Superdex 200 prep grade column (GE Healthcare Life Sciences) and eluted with buffer containing 20 mM Tris-HCl, pH 7.9, 100 mM NaCl, 1 mM dithiothreitol. The final product was concentrated to 5 mg/ml maintained in 20 mM Tris-HCl, pH 7.9, 100 mM NaCl, with 20% glycerol, divided into small aliquots, and stored at -30 °C. The protein concentration was determined by bicinchoninic acid (BCA) method (16).

Enzyme Assay—The NTP-PPase activity of MazG was assayed by measuring the hydrolyzed product, PP_i, by an enzyme-coupled colorimetric assay (Molecular Probes) with detection limit of 0.2 μ M (17). The standard NTP-PPase assay was carried out in 20 μ l reaction buffer (50 mM glycine-NaOH, pH 9.6, 100 mM NaCl, 5 mM Mg²⁺) containing 1 μ g of MtMazG and appropriate amount of nucleoside triphosphates at 37 °C for 10 min. The reaction was stopped by heating at 70 °C for 10 min, and 5 μ l of reaction product was applied for PiPer pyrophosphate assay (Molecular Probes) according to the manufacturer's instructions in the “Assaying for Pyrophosphate” setting. The reaction without MtMazG or substrates was carried out as a background control. Reaction conditions including temperature, pH, Mg²⁺ concentration, amount of MtMazG and reaction time, were optimized (supplemental Fig. S1). To optimize the pH, both the Tris-HCl buffer for pH 6.8–8.8, and the glycine-NaOH buffer for pH 9.2–11.0 were used.

CD Spectrometry—The CD (circular dichroism) spectra were measured on a Jasco J-715 spectropolarimeter in the far-ultraviolet region (260–190 nm) in steps of 1 nm. Records on protein solutions (20 μ g/ml in H₂O) employing a cell with path length of 1 cm at 18 °C were obtained. The mean residue ellipticity, represented in millidegrees, was calculated using a mean residue molecular mass of 110 Da. To see the CD spectra changes upon addition of Mg²⁺, MgCl₂ solution was added to the protein samples immediately before measurement. Each spectrum reported is an average of five scans. Blank spectra of aqueous buffer were used to correct the observed spectra.

Construction of *mazG*-null Mutant and Complementation in *M. smegmatis mc*² 155—The following procedures were carried out to construct the Δ *mazG*::*hyg* null mutation in *M. smegmatis mc*² 155 (18). Two homology arms (0.83 kb and 0.99 kb for left and right arm, respectively) overlapping the *mazG* gene at its 75 and 99 extremities were PCR-amplified from genomic DNA by using primers MKO1/MKO2 and MKO3/MKO4, respectively. The PCR products were digested and cloned into the cosmid

MtMazG Is a Novel NTP-PPase Involved in Oxidative Response

vector pYUB854 in their original genome orientation separated by the *res-hyg-res* cassette. The resulting cosmid was digested by *PacI* and inserted into the genome of mycobacteriophage phAE87 and was subsequently packaged by the Packagene® Lambda DNA Packaging System (Promega). The recombinant transducing phage was used to construct the *mazG*-null mutant. The dUTP-biotin labeled probe (Fermentas) was used for Southern blot analysis of the *PstI* digested chromosomal DNA on the Hybond-N⁺ nylon membrane (GE Amersham Biosciences), according to the standard method (19).

For complementation of the *mazG* mutant in *M. smegmatis*, *mazG* gene from H37Rv, H37Ra, *M. smegmatis* and *E. coli* were PCR-amplified using the primers CTBF/CTBR (for both H37Rv and H37Ra), CMSF/CMSR, and CECF/CECR, respectively. The native promoter region (425 bp region from 5509332 to 5509756 of *M. smegmatis* genome, see supplemental Fig. S2) of the *mazG* operon was amplified with the primers ProF/ProR. The PCR products were enzyme digested and subsequently cloned into the integrative plasmid pMV306. The resulting plasmids containing the *mazG* gene under control of its native promoter were used to complement the *M. smegmatis mazG*-null mutant.

Survival Assay under Oxidative Stress—*M. smegmatis* strains were grown in 7H9 broth supplemented with 0.2% glycerol and 0.05% Tween 80 at 37 °C. For determination of survival following hydrogen peroxide (H₂O₂) exposure, log phase cultures (*A*₆₀₀ at 0.4–0.5) were diluted in fresh medium to an *A*₆₀₀ of 0.2, and exposed to 5 mM hydrogen peroxide (20). Cultures were incubated by rolling at 37 °C, and aliquots were removed from each culture for plating at the indicated time points. Colonies were counted after 3 days by plating in triplicate at three dilutions onto 7H11 plates containing appropriate antibiotics.

Quantitative Real-time PCR—RNA was extracted from H₂O₂-treated and untreated log phase cultures (*A*₆₀₀ ~0.5) using the RiboPure-Bacteria kit (Ambion). cDNA was synthesized using the SuperScript III First Strand kit (Invitrogen) with random hexamers primer. Target gene transcript levels in H₂O₂-treated log phase cultures were measured by quantitative real-time PCR with SYBR Green as label, normalized to *sigA* transcript levels (21), and expressed as a fold change from untreated cultures.

Analytical Gel Filtration—Hiload 16/60 Superdex 200 per grade column (GE Healthcare Life Sciences) was employed to determine the molecular mass of MazG. The sample was eluted by 50 mM phosphate buffer, pH 8.0, 150 mM NaCl, flow rate was set to 1 ml/min and elution of the protein was monitored at 280 nm. Aldolase (158 kDa), bovine serum albumin (67 kDa), ovalbumin (43 kDa), and chymotrypsinogen A (25 kDa) were taken for calibration.

RESULTS

Cloning, Expression, and Purification of MazG from *M. tuberculosis*, *M. smegmatis*, and *E. coli*—The *mazG* genes containing the sequence of either the prototype H37Rv (Rv1021) or the mutated H37Ra (MRA_1029) were cloned into plasmid pET22b(+) and expressed in *E. coli* BL21(DE3) cells. The His-tagged MazG proteins (36.3 kDa) eluted from the nickel-affinity column were subsequently purified by Superdex 200 chroma-

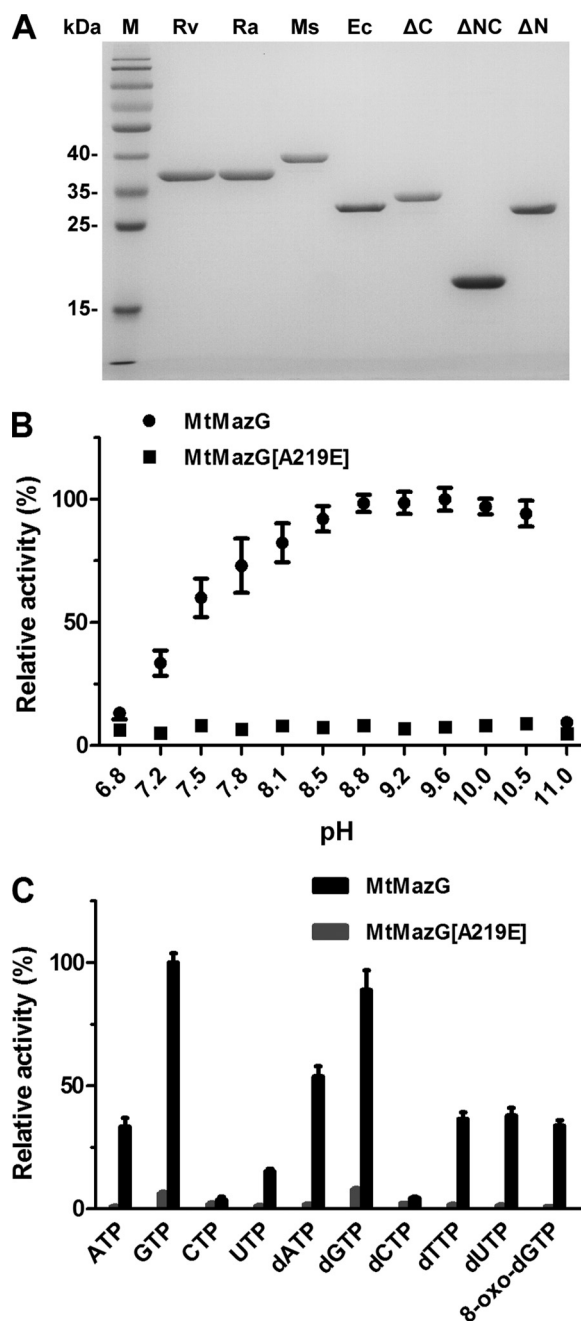


FIGURE 1. Enzymatic properties of MtMazG. A, purified recombinant MazG proteins expressed in *E. coli*. Proteins were expressed and purified as described in "Experimental Procedures." The protein purity was analyzed by 12% SDS-PAGE, about 1 μ g of purified proteins were loaded. Rv, Ra, Ms, and Ec stand for H37Rv, H37Ra, *M. smegmatis* and *E. coli* MazG, respectively; Δ C, Δ N, and Δ NC stand for the C-terminal region, NE region, and dual-region truncated variants of MtMazG. B, optimal pH curve for MtMazG reactions. Reactions were conducted as described in "Experimental Procedures" with 1 mM GTP as substrate. The hydrolysis activity under each pH was normalized to the activity of that under pH 9.6 (100%, correspond to PPI formation ability of $600 \pm 40 \mu\text{M}/10 \text{ min}$). C, substrate specificity of MtMazG. Relative hydrolysis activities toward various substrates (1 mM) at standard condition were normalized to that of GTP (100%, the same as panel B). All data were the mean \pm S.E. from at least four independent experiments.

tography to nearly SDS-PAGE homogeneity. The EcMazG and the MsMazG (MSMEG_5422), including the truncated variants of MtMazG (see following), were all similarly expressed and purified (Fig. 1A).

TABLE 1

Kinetic parameters of MazG proteins analyzed in this study

Standard reaction assay was performed as described in "Experimental Procedures." Kinetic parameters were determined with eight different concentrations of each substrate ranged from 0.1 to 2 mM (0.03–1.5 mM for 8-*oxo*-dGTP). Values represent the mean \pm S.E. of four independent experiments. Kinetic parameters for all tested substrates of MsMazG are listed in supplemental Table S2.

Species	Enzyme	Mg ²⁺	Substrate	V _{max}	k _{cat}	K _m	k _{cat} /K _m	
		mM		nm/min/μg	min ⁻¹	mM	min ⁻¹ mM ⁻¹	
Mt	WT	5	GTP	1.5 \pm 0.1	55.2 \pm 3.1	0.4 \pm 0.1	139	
	WT	5	dGTP	1.4 \pm 0.1	51.8 \pm 2.1	0.4 \pm 0.1	130	
	WT	5	dATP	1.7 \pm 0.2	60.4 \pm 7.2	1.2 \pm 0.3	52	
	WT	5	dTTP	1.6 \pm 0.1	58.4 \pm 3.9	1.3 \pm 0.2	44	
	WT	5	dUTP	1.2 \pm 0.2	45.3 \pm 6.0	1.1 \pm 0.3	43	
	WT	5	ATP	1.3 \pm 0.1	48.4 \pm 5.1	1.6 \pm 0.3	31	
	WT	5	UTP	0.5 \pm 0.04	16.8 \pm 1.5	0.6 \pm 0.2	26	
	E219	5	GTP	0.08 \pm 0.01	2.8 \pm 0.2	0.3 \pm 0.1	10	
	WT	20	GTP	2.3 \pm 0.2	85.5 \pm 6.4	0.6 \pm 0.1	134	
	E219	20	GTP	0.8 \pm 0.1	30.7 \pm 3.7	1.2 \pm 0.3	29	
	WT	5	8- <i>oxo</i> -dGTP	0.14 \pm 0.01	5.2 \pm 0.2	0.11 \pm 0.02	47	
	E219	5	8- <i>oxo</i> -dGTP	ND ^a	ND	ND	ND	
	Ms	WT	5	GTP	3.1 \pm 0.2	115 \pm 6.2	0.9 \pm 0.1	127
		E222	5	GTP	0.11 \pm 0.02	4.1 \pm 0.6	0.9 \pm 0.3	4
WT		5	8- <i>oxo</i> -dGTP	0.16 \pm 0.01	5.9 \pm 0.2	0.16 \pm 0.02	36	
E222		5	8- <i>oxo</i> -dGTP	ND	ND	ND	ND	
Ec	WT	5	dATP	1.9 \pm 0.1	59.8 \pm 2.3	0.34 \pm 0.05	174	
	E141	5	dATP	1.8 \pm 0.1	57.8 \pm 2.4	0.37 \pm 0.05	156	
	WT	5	dUTP	1.9 \pm 0.1	60.3 \pm 3.1	0.71 \pm 0.1	85	
	WT	5	8- <i>oxo</i> -dGTP	0.23 \pm 0.01	7.2 \pm 0.4	0.36 \pm 0.05	20	
	E141	5	8- <i>oxo</i> -dGTP	0.22 \pm 0.01	6.9 \pm 0.3	0.42 \pm 0.06	17	

^a ND, nondetectable.

The NTP-PPase Activity of MtMazG and MsMazG—The NTP-PPase activity was assayed by measuring the PP_i product, which was first converted to P_i by inorganic pyrophosphatase, and the P_i level was subsequently quantified by an enzyme coupled colorimetric method (see "Experimental Procedures"). Like other characterized MazG proteins (10, 22, 23), MtMazG was found to maintain more than 70% of its NTP-PPase activities between pH 7.8 and 10.5, with the optimum pH at 9.6 (Fig. 1B). Mg²⁺ acted as an optimal cofactor among the 7 divalent cations tested in our assay (supplemental Fig. S1A). The NTP-PPase activity of MtMazG was the highest at 37 °C and nearly abolished at 70 °C. The effects of pH and temperature on protein stability were also examined. Incubation of the enzyme in pH 9.6 at 37 °C for 10 min did not affect its NTP-PPase activity (supplemental Fig. S1B).

The general kinetic parameters of MtMazG were determined using 8 canonical (d)NTPs as the substrates (Table 1). It was found that MtMazG converted all of the tested substrates into their nucleoside monophosphate derivatives and PP_i. No detectable P_i formed because the reaction strictly depended on inorganic pyrophosphatase. Of (d)NTPs examined, GTP and dGTP were the most preferred substrates for MtMazG (Fig. 1C), with K_m values of 0.4 \pm 0.06 mM for either of them, which is 1.5–4 times lower than that of other substrates. On the other hand, the CTP and dCTP hydrolysis activities of MtMazG were too low to allow for determination of their kinetic parameters (Fig. 1C). As shown, MsMazG exhibited the same optimal reaction conditions and substrate spectrum relative to MtMazG (Tables 1 and supplemental Table S2), indicating that MsMazG is functionally similar to MtMazG.

dUTP and 8-oxo-dGTP Hydrolysis Activity of Mt-, Ms-, and EcMazG—It is noteworthy that MtMazG and MsMazG are able to hydrolyze dUTP (Table 1), the most common mutagenic NTP produced as a byproduct during thymine

nucleotide biosynthesis (9, 24). Both enzymes exhibited a moderate affinity toward dUTP with a K_m of ~1 mM, similar to most of their tested canonical NTP substrates and of their homolog from *Thermotoga maritima* (23, 25). EcMazG is capable of hydrolyzing dUTP as well. Although it exhibits lower substrate affinity (with a K_m of 0.7 mM) than that with canonical NTP substrates (Table 1), it is comparable to or better than that of MtMazG.

Given that MtMazG can hydrolyze dUTP, we subsequently tested the hydrolysis activity of MtMazG toward 8-*oxo*-dGTP, a major mutagenic substrate for DNA synthesis arising from oxidative damage (Table 1) (26–28). It was found that both MtMazG and MsMazG exhibited substantially high substrate affinity to 8-*oxo*-dGTP, with a K_m of 0.11 and 0.16 mM, respectively. The K_m value for 8-*oxo*-dGTP hydrolysis reaction of EcMazG was 0.36 mM, which is not significantly different from that with other substrates (Table 1). The order of k_{cat}/K_m for Mt-, Ms, and EcMazG is: 47, 36, and 20 min⁻¹mM⁻¹, respectively.

The A219E Mutation in MtMazG Nearly Abolishes Its NTP-PPase Activity—Under the aforementioned optimal conditions for MtMazG, the hydrolytic activities of MtMazG[A219E] were examined using various substrates (Table 1 and Fig. 1C). MtMazG[A219E] hydrolyzed GTP with k_{cat} that is 20-fold lower than that of the wild type. However, the mutant enzyme K_m is reduced about 25% relative to that of MtMazG. Thus, the catalytic efficiency of MtMazG[A219E] is down to 7% of the wild-type level (Fig. 2B and Table 1). The same results were obtained from the experiments performed at a range of pH 6.8–11 (Fig. 1B). In addition, the corresponding mutation (A222E) in MsMazG resulted in a decrease of the hydrolysis activity to levels similar to those observed with the A219E mutation in MtMazG, suggesting that MsMazG and MtMazG share similar catalytic mechanism. No detectable 8-*oxo*-dGTP hydrolysis activities were observed with either MtMazG[A219E]

MtMazG Is a Novel NTP-PPase Involved in Oxidative Response

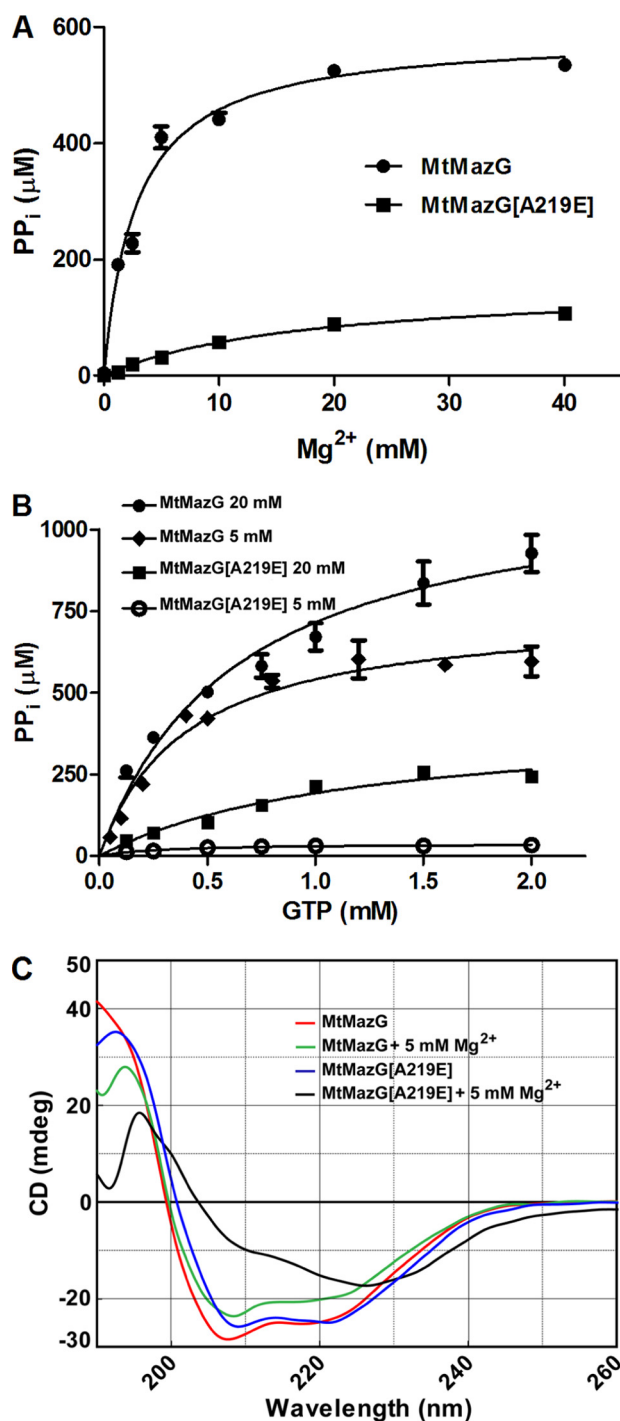


FIGURE 2. Mg²⁺ requirement and CD spectrum study of MtMazG and MtMazG[A219E]. A, Mg²⁺ concentration-dependent activation of MtMazG and MtMazG[A219E]. With 0.5 mM GTP as substrate, the PP_i formation ability (μM/10 min) of the MtMazG[A219E] variant and its prototype enzyme was monitored under increased Mg²⁺ concentration. The reaction mixture without substrates was used as a background control. B, Michaelis-Menten curves for MtMazG and MtMazG[A219E] under 5 mM and 20 mM Mg²⁺. GTP was chosen as substrate and its concentration were depicted. Each value (μM/10 min) is the mean ± S.E. from three independent experiments. C, CD spectra of MtMazG and MtMazG[A219E] measured at 18 °C in the presence or absence of 5 mM Mg²⁺. CD spectra with 10 or 15 mM Mg²⁺ exhibited a similar CD spectrum to that observed with 5 mM Mg²⁺. Each spectrum reported is an average of five scans.

or MsMazG[A222E], indicating that this mutation reduced 8-oxo-dGTP hydrolysis activity by a factor of greater than 35 times (Table 1).

A219E Mutation in MtMazG Affects Mg²⁺ Binding and Protein Structure—Residue Ala-141 of the EcMazG (corresponding to Ala-219 of MtMazG) is located near the catalytic center motif for Mg²⁺ and substrate binding (11), we reasoned that the A219 → E substitution of MtMazG might result in an increase of negative charge that alters Mg²⁺ binding. As revealed by the Mg²⁺ titration experiments, Mg²⁺ activated both MtMazG and MtMazG[A219E] (supplemental Fig. S3), while the MtMazG[A219E] exhibited a K_{act} for Mg²⁺ of 17.4 ± 4 mM, which is six times higher than that for MtMazG (2.8 ± 0.3 mM) (Fig. 2A). Increasing Mg²⁺ concentration from 5 to 20 mM enhanced the MtMazG[A219E] V_{max} for the formation of PP_i by nearly 10-fold (Fig. 2B and Table 1). However, even at 20 mM Mg²⁺, A219E exhibited the catalytic efficiency at levels no more than 25% of the wild type (Fig. 2B).

Given that MtMazG A219 is essential for catalysis but is unlikely located in the catalytic center, we suspect that it may play an important role in determining the overall conformation of the protein. To address this possibility, we performed CD spectra analysis with purified MtMazG and MtMazG[A219E] in the presence or absence of Mg²⁺. In the absence of Mg²⁺, both the wild type and the mutant enzyme exhibited a similar pattern of α -helices and β -strands (Fig. 2C). These results are consistent with the CD spectra pattern observed with the MazG family proteins in the previous studies (10, 25), suggesting that MtMazG and MtMazG[A219E] share nearly identical structures in the absence of Mg²⁺. However, whereas the addition of 5 mM Mg²⁺ resulted in minor changes in the CD spectra of the wild-type enzyme, it induced significant alterations to the A219E protein (Fig. 2C). Similar observations were made with the wild type and A219E in the presence of 10 or 15 mM Mg²⁺ (data not shown). These results suggest that upon Mg²⁺ binding, the negative charge of the E219 side chain induces rather drastic alterations in the secondary structures of MtMazG, and this altered conformation may explain the severe deficiency of MtMazG[A219E] in hydrolysis.

MazG Is Required for Full Oxidative Stress Response in M. smegmatis—To explore the *in vivo* function of MtMazG and evaluate the physiological effect of A219E mutation, we constructed a $\Delta mazG::hyg$ null mutation in the fast-growing *M. smegmatis* mc² 155, which was confirmed by Southern blot (Fig. 3B). The wild-type and *mazG*-null strains were subject to oxidative stress, elicited by exposure to 5 mM H₂O₂ (20, 29). Nearly 80% of the wild-type bacteria were viable after the treatment for 1 h, whereas only 40% of the mutant bacteria survived under the same condition (Fig. 3C), revealing a defect for the *mazG*-null mutant in response to oxidative stress. This 2-fold decrease in viability by the *mazG* mutant under oxidative stress is significant, as comparable effect was observed on mycobacterial *sigI*, *sigE* and *ppk* mutants in previous publications (29–31). Importantly, the attenuated phenotype in the *mazG*-null mutant can be fully complemented by the expression of the wild-type *mazG* gene of *M. smegmatis* under its native promoter (the characterization of the *mazG* operon and its promoter region is shown in supplemental Fig. S2).

Of note, the *mazG*-null mutant showed no growth defects *in vitro* (supplemental Fig. S4). Moreover, no difference was observed between the wild-type and *mazG*-null *M. smegmatis* under starva-

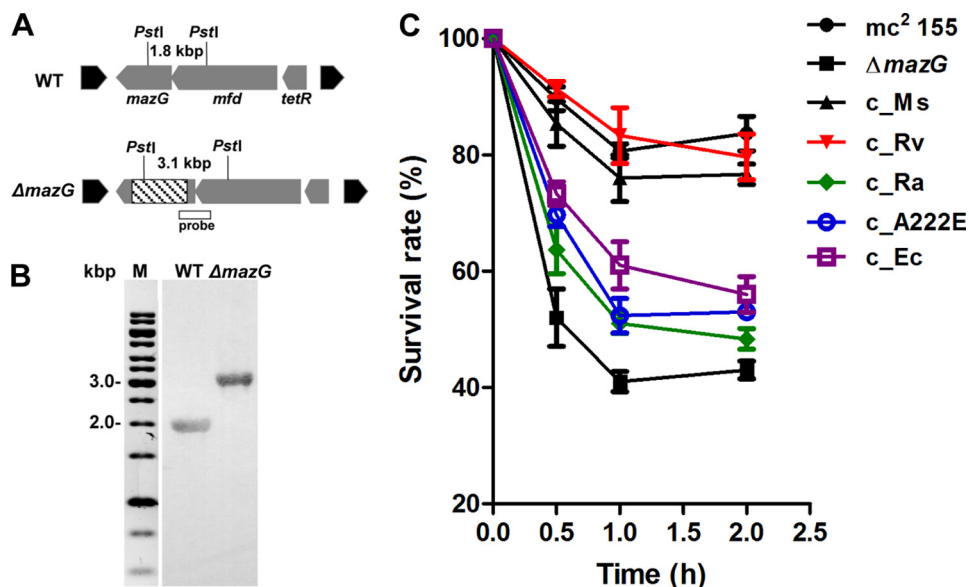


FIGURE 3. Southern blot analysis and phenotypic characterization of *mazG* mutant in *M. smegmatis*. *A*, schematic diagrams of WT and the *mazG*-deleted ($\Delta mazG$) loci. The putative *mazG* operon (gray arrows) and its adjacent genes (black arrows) are depicted. The expected sizes for the restriction enzyme, *Pst*I and the probe fragment used for Southern blot are as shown. *B*, Southern blot analysis of the WT and $\Delta mazG$ strains. A dUTP-biotin labeled fragment was used to probe *Pst*I-digested chromosomal DNA separated by 0.8% agarose gel. Lane *M* contains a 1-kb DNA ladder (Fermentas). *C*, survival abilities under oxidative stress exerted by 5 mM H_2O_2 . The strains used in this assay are wild type (mc^2 155), *mazG* mutant ($\Delta mazG$), and strains complemented by MsMazG (*c_Ms*), MtMazG (*c_Rv*), MtMazG[A219E] (*c_Ra*), MsMazG[A222E] (*c_A222E*), and EcMazG (*c_Ec*). The starting CFU of this survival assay was around $1 \sim 2 \times 10^7$ (100%). All data were the mean \pm S.E. from four independent experiments.

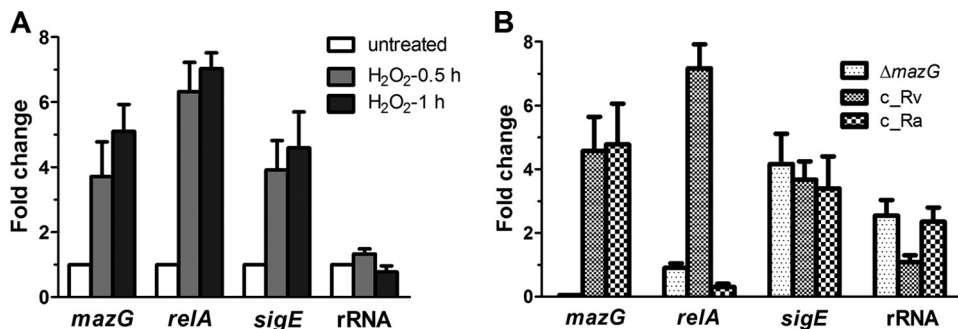


FIGURE 4. Mycobacterial *mazG* is an oxidative stress-inducible gene and its NTP-PPase activity is required for induction of *relA* upon oxidative insult. qRT-PCR was used to measure target gene mRNA level in H_2O_2 -treated log phase cultures. Transcript levels were normalized relative to *sigA*, and expressed as a fold change from untreated cultures. *A*, oxidative stress-induced transcript levels of *mazG*, *relA*, *sigE*, and 16 S rRNA in wild-type *M. smegmatis*. *B*, transcript levels of *mazG*, *relA*, *sigE*, and 16 S rRNA in *mazG*-null mutant ($\Delta mazG$), and strains complemented with MtMazG[A219E] (*c_Ra*) or MtMazG (*c_Rv*), which were treated by 5 mM H_2O_2 for 30 min. All data were presented as mean \pm S.E. from at least three independent experiments.

tion conditions (log-phase bacteria were placed in phosphate-buffered saline for 30 days (32)) (data not shown). This finding suggests that mycobacterial *mazG*, unlike its counterpart in *E. coli* (8), is not required for starvation response. Taken together, these results suggest that *mazG* is specifically required for *M. smegmatis* full capacity to respond to oxidative stress.

The Oxidative Stress-Response Property of MtMazG Is Dependent on Its NTP-PPase Activity—The *mazG* fusion genes from H37Rv and H37Ra under control of the native *mazG* promoter from *M. smegmatis* were separately integrated into the *attB* sites of the *mazG*-null mutant strain of *M. smegmatis*. As with MsMazG complementation, H37Rv *mazG* fully restored the ability of the mutant strain to survive under oxidative stress. However, expression of MtMazG[A219E] under the same con-

dition improved cell viability only slightly (Fig. 3C). Similarly, the introduction of MsMazG[A222E], equivalent to the MtMazG[A219E], failed to complement (Fig. 3C). Thus, the NTP-PPase activity is required for Mt- or MsMazG to mediate full cellular response to oxidative stress.

Interestingly, in contrast to Mt- or MsMazG, EcMazG only marginally complement the *mazG*-null mutant (Fig. 3C). These findings suggest that MazG-mediated cellular response to oxidative stress is specific to mycobacteria.

Transcription of *mazG* Is Up-regulated under Oxidative Stress, and Induction of *relA* Is Repressed in *mazG*-null or MtMazG[A219E] Mutant—Quantitative real time PCR was used to investigate transcriptional changes of *mazG* under oxidative stress. It was found that expression of *sigE* and *relA*, two regulatory genes involved in oxidative stress response (30, 33), were increased about 3.9 and 6.3 times, respectively, after exposure to 5 mM H_2O_2 for 0.5 h (Fig. 4A). Transcription of *mazG* was up-regulated 3.7 times and 5.1 times after the treatment for 0.5 and 1 h, respectively (Fig. 4A), indicating that *mazG* is an oxidative stress response gene.

The *sigE* and *relA* mRNA levels in *mazG*-null mutant were also measured. Surprisingly, while the transcriptional activation of *sigE* under oxidative stress remained unchanged in the *mazG*-null strain, the induction of *relA* is severely repressed after exposure to H_2O_2 for 0.5 h (Fig. 4B). Consistent with

this observation, the expression of 16 S RNA, a well known target for repression by RelA-mediated stringent response (34), was found up-regulated only in the *mazG* mutant strain under oxidative stress (Fig. 4B). Moreover, expression of MtMazG, but not the H37Ra-derived MtMazG[A219E], in *mazG* mutant strain restored *relA* transcription to the level of wild type (Fig. 4B). These results establish that induction of *relA* under oxidative stress is dependent on the NTP-PPase activity of mycobacterial MazG.

MtMazG Is Structurally Different from EcMazG—We investigated structural differences that may underlie the seemingly differential physiological functions exhibited by MtMazG and EcMazG. It was reported that EcMazG is composed of two core MazG domains connected in tandem, termed the N- and the

MtMazG Is a Novel NTP-PPase Involved in Oxidative Response

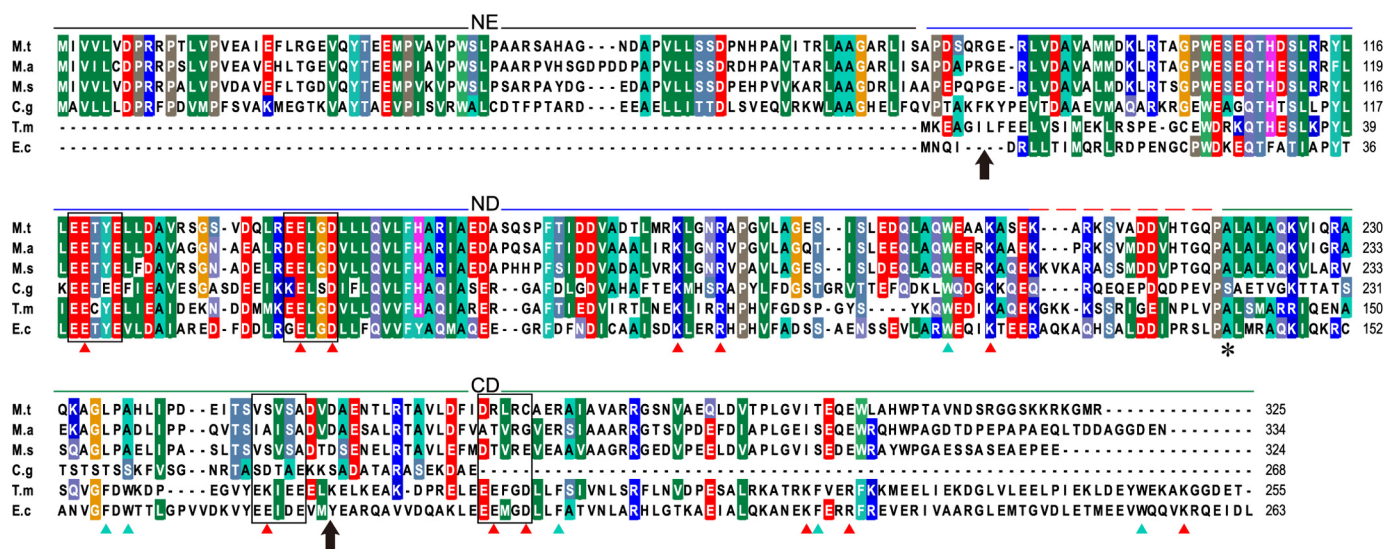


FIGURE 5. **Sequence alignment of MazG proteins.** The sequences are from *M. tuberculosis* H37Rv (*M.t*), *M. avium* 104 (*M.a*), *M. smegmatis* mc²155 (*M.s*), *Corynebacterium glutamicum* ATCC 51867 (*C.g*), *T. maritima* MSB8 (*T.m*), and *E. coli* MG1655 (*E.c*). The N-terminal (NE) and C-terminal domains (CD) of EcMazG and the N-terminal extra region (NE) of MtMazG are indicated. Four EEXX (E/D) motifs from EcMazG are indicated by blank rectangles. Key residues of EcMazG involved in Mg²⁺ coordination and substrates binding are indicated by red and cyan triangles, respectively (11). The Ala-219 residue is marked with an asterisk. Black arrows indicate the truncation sites for NE region and C-terminal region.

C-terminal domains (11). Sequence comparison indicated that MtMazG had an extra N-terminal 80 residues (NE region) relative to that of EcMazG (Fig. 5). Furthermore, it seems that MtMazG only has one region highly homologous to the N-terminal domain of EcMazG, which contains key residues required for Mg²⁺ coordination and substrate binding. However, the MtMazG C terminus is unlike composed of a MazG-like core domain because secondary structure predictions reveal that this region contains only two α -helices, whereas a typical MazG-like core domain consists of five α -helices (10, 22). Taken together, MtMazG appears to organize by a single MazG-like core domain that is flanked with an N-terminal and a C-terminal region with unknown functions.

It has been shown that MazG proteins with a single core domain form tetrameric structures, whereas an analog with two core domains is dimeric (10, 11, 22). To determine the stoichiometric composition of MazG oligomer, MazG from different species were subject to size exclusion chromatographic analysis. MtMazG was eluted as a single species with a partition coefficient value (K_{av}) of 0.35, corresponding to the molecular mass of ~140 kDa, while EcMazG was eluted as a dimer with a molecular mass of ~64 kDa (K_{av} = 0.44) (Fig. 6A). These results suggest that MtMazG is a tetrameric complex under native conditions, which further supports the hypothesis that MtMazG contains a single core MazG domain.

Although MtMazG is structurally different from EcMazG, the A219 residue of MtMazG is conserved in the EcMazG protein. The corresponding A141E substitution protein of EcMazG (EcMazG[A141E]) was expressed and purified to nearly homogeneity (Fig. 1A), and its enzymatic activity was assayed as described (23). With dATP as the substrate, EcMazG[A141E] exhibited the wild-type level of NTP-PPase activity (Fig. 6C and Table 1). Its K_m value was 9% higher than that of the wild-type enzyme, while the V_{max} remained unchanged. Altogether, the above results suggest that the MtMazG and the EcMazG differ

substantially in their overall structures and the catalytic mechanisms.

The NE and C-terminal Regions of MtMazG Are Essential for NTP-PPase Activity—To study the functions of the NE and C-terminal regions of MtMazG, we performed deletion analysis by constructing MtMazG Δ N (corresponding to residues 84–325; 27.7 kDa), MtMazG Δ C (corresponding to residues 1–253; 27.9 kDa), and MtMazG Δ NC (corresponding to residues 84–253; 19.8 kDa) (Fig. 5). The deletion sites were selected according to the following criteria. 1) The deleted regions should not exceed the target domains. 2) The truncation sites should not interrupt secondary structure elements, especially helices. 3) If possible, the deleted regions should not be conserved among MazG family proteins.

These truncated MtMazG proteins were expressed and purified (Fig. 1A). These truncations did not affect protein yields or solubility, and the tetrameric structures were well retained as shown by the size exclusion chromatographic analysis (Fig. 6B). However, no NTP-PPase activity was observed with any of three truncated proteins in the presence of GTP or 8-*oxo*-dGTP as substrate. These results suggest that both the MtMazG NE region and C-terminal region are essential for the NTP-PPase activity.

DISCUSSION

In this study, we characterized a novel MazG protein from *Mycobacterium*, a genus of the *Actinobacteria* phylum. The mycobacterial MazG appears to differ structurally and functionally from its homologs characterized to date, including MazG from *E. coli* (8, 23), *T. maritima* (25), *Vibrio* sp (22), and *Mus musculus* (designated RS21-C6) (35). Size exclusion chromatographic analysis demonstrated that the MtMazG forms a tetrameric structure with each subunit containing a single core MazG domain flanked by two additional regions (or domains). Both of these flanking regions are essential for the hydrolysis

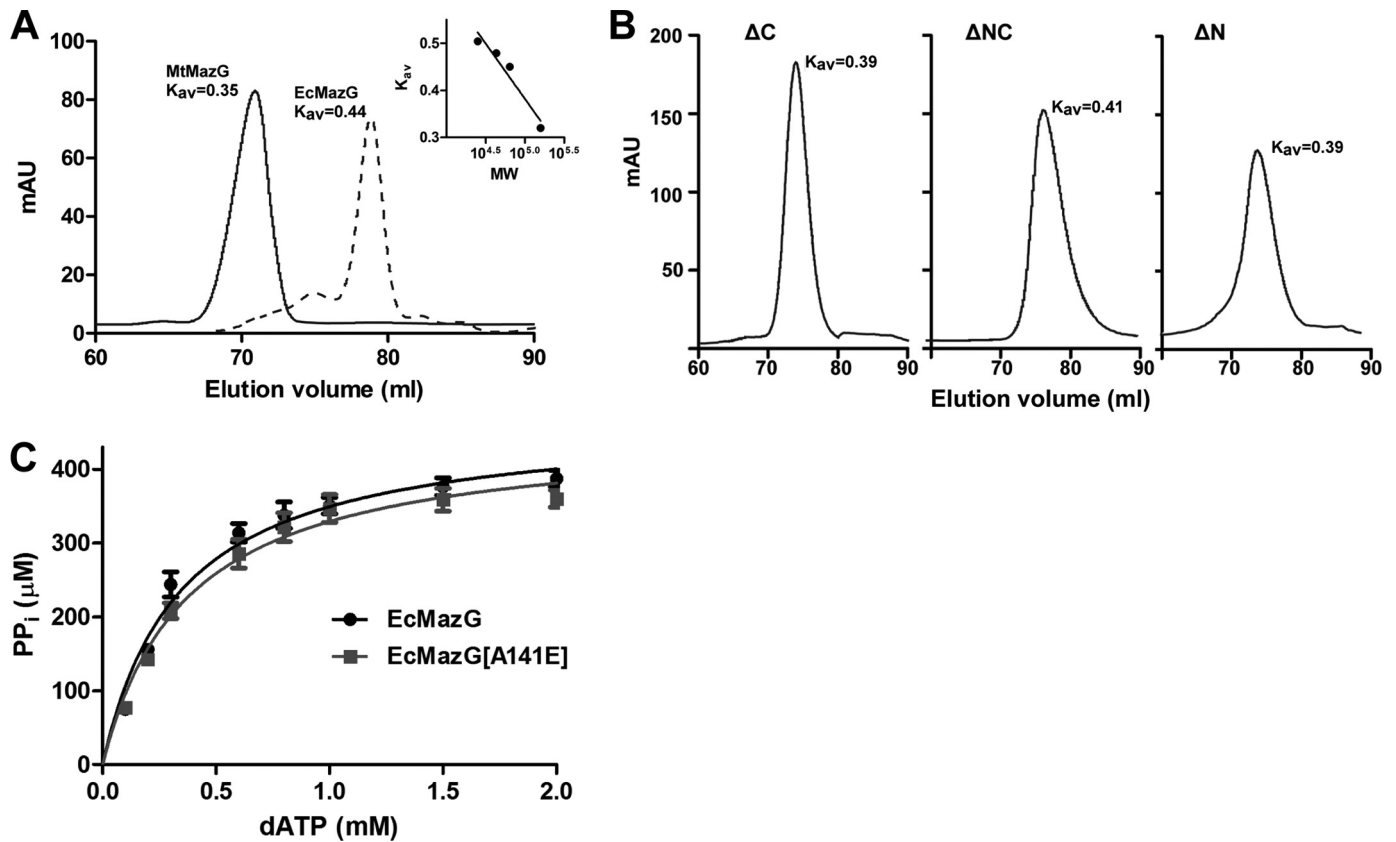


FIGURE 6. **MtMazG is structurally different from EcMazG.** *A*, size exclusion chromatographic analysis of MtMazG (solid) and EcMazG (dashed). Two independent elution curves are overlaid with K_{av} value for each peak indicated. The calibrated curve is shown in the inset. *B*, size exclusion chromatographic analysis for the oligerization conformation of MtMazG mutants with deletions in the NE region (ΔN), C-terminal region (ΔC), or dual-regions (ΔNC). The ΔN and ΔC exhibited an apparent molecular mass of ~ 106 kDa, whereas ΔNC is about 84 kDa. *C*, Michaelis-Menten curves for EcMazG and its A141E variant. The assay was conducted as described previously (23). dATP was used as substrate with eight different concentrations ranging from 0.1 to 2.0 mM. Each value ($\mu M/10$ min) is the mean \pm S.E. of three independent experiments.

Type	Dominant domain organization ^a	Phylum (occurrence) ^b	Characterized example	Physiological role
I	MazG	Widespread	<i>Vibrio sp</i>	NA ^c (22)
II	UK-MazG-UK	Actinobacteria (45%)	<i>M. tuberculosis</i>	oxidative response and putative house cleaning (this work)
	MazG-UK	Actinobacteria (35%)	NA	NA
III	MazG-MazG	Bacteroidetes (86%)	NA	NA
	MazG-MazG	Proteobacteria (80%)	<i>E. coli</i>	regulation of ppGpp (8). putative house cleaning (this work)
IV	M-MazG-MazG	Thermotogae (100%)	<i>T. maritima</i>	NA (25)
	M-MazG-MazG	Firmicutes (50%)	NA	NA

a. Dominant domain organization (>85%) in each type. UK, unknown function; M, methylase domain.
 b. Occurrence of this domain relative to the number of genus of indicated phylum
 c. Not available

FIGURE 7. **Domain associations of MazG family proteins and their relationships to species evolution.** MazG family proteins from 832 species were selected for analysis based on protein sequence homology. Dominant domain associations in each type are depicted, and their occurrence relative to total genus number is illustrated.

activity, as deletion of either leads to complete loss of NTP-PPase activity. This structural feature distinguishes MtMazG from all other currently characterized MazG family proteins (9, 10, 22). We found that nearly 80% of MazG homologs from *Actinobacteria* exhibited the MtMazG-like domain organization (Fig. 7), whereas in other phyla, such configuration is rarely observed.

Genome-wide analysis of the MazG family proteins from 832 species has led us to classify them into I-IV major subgroups based on their determined/predicted structural organizations (Fig. 7 and supplemental Table S3). Type I, represented by *iMazG* from *Vibrio sp* (22), contains a single MazG core domain. Type II, found predominantly in *Actinobacteria*, is composed of a single core MazG domain and one or two flanking regions. It has two subclasses depending on

MtMazG Is a Novel NTP-PPase Involved in Oxidative Response

whether it contains either both N- and C-terminal flanking regions or a single C-terminal segment. Type III has double core-domain in tandem and is found in *Proteobacteria*. Finally, in *Firmicutes*, type IV is organized by a double core-domain in tandem and a methylase domain at the N terminus.

MazG family proteins are long believed to function as house-cleaning enzymes involved in degrading non-canonical NTPs, such as dUTP, 8-*oxo*-dGTP and other mutagenic NTPs, and thus preventing their incorporation into DNA or RNA (9, 10, 22). However, direct evidence supporting this putative function is lacking. In this study, we showed, for the first time, that MtMazG and EcMazG can hydrolyze both dUTP and 8-*oxo*-dGTP (Table 1). MtMazG exhibited a K_m of 0.11 mM toward 8-*oxo*-dGTP, suggesting a role for this enzyme to recognize the damaged nucleotide preferentially in comparison to canonical NTPs. However, this affinity is about 230-fold lower than that exhibited by *E. coli* MutT, which hydrolyzes 8-*oxo*-dGTP with a K_m of 0.48 μ M (36). It thus appears unlikely that 8-*oxo*-dGTP is a physiological substrate of MtMazG. Given that only a few out of more than 20 different types of damaged nucleotides have been discovered are available (37), it remains a daunting challenge to identify the MtMazG physiological substrate(s) by *in vitro* enzyme assay at the present time. Despite the lack of physiological substrates, our current study has advanced the understanding of the function of mycobacterial MazG by linking this enzyme to cellular regulatory pathway in response to oxidative stress. We have shown that in *M. smegmatis*, MazG is an oxidation-inducible gene product (Fig. 4) that is required for the full capacity of mycobacteria to respond to oxidative stress (Fig. 3C). These observations are in line with the house-cleaning hypothesis, suggesting that mycobacterial MazG, induced by oxidative stress, could conceivably act to degrade the oxidation-induced damaged nucleotides. Impairment of such hydrolysis activity would compromise cell viability, which was observed in *M. smegmatis* that was deleted of MazG or expressed a mutant form of MazG (MtMazG[A219E]) with poor catalytic function (Fig. 3C).

Another interesting finding of our study is that induction of *relA* under oxidative stress is dependent on the NTP-PPase activity of mycobacterial MazG (Fig. 4B). This observation is in agreement with a previous report that *E. coli* MazG-mediated, starvation-induced programmed cell death was associated with altered cellular ppGpp levels (8), suggesting an interplay between EcMazG and RelA. As a key player in stress-induced physiological adaptation (34), RelA is required for mycobacterial survival under *in vitro* starvation and hypoxia conditions, as well as long-term persistence of *M. tuberculosis* in mice (32, 38). Therefore, RelA dysfunction may affect bacterial survival under stress conditions as observed in the *mazG*-null mutant. However, although RelA is involved in oxidative response, the *relA*-deleted *M. smegmatis* did not show survival defect under oxidative stress (32, 39). This suggests that induction of *relA* may not be required for cellular oxidative stress response directly. Alternatively, redundant RelA-independent pathways might be sufficient for cellular oxidative stress response under the experimental conditions. It is also possible that RelA is involved in adaptation following oxidative stress. It is worth noting that mycobacterial and *E. coli* MazG appear to act dif-

ferently in cellular stress response. We have shown that in contrast to mycobacterial MazG, EcMazG cannot complement *M. smegmatis mazG*-null mutant in response to oxidative stress (Fig. 3C). However, unlike EcMazG (8), MsMazG is not required for cell viability under the starvation conditions (data not shown).

We have validated our previous prediction (2) that the A219E substitution in H37Ra MazG is a loss-of-function mutation both *in vitro* and *in vivo*. Whereas it remains to be elucidated how the A219E substitution inactivates the MazG hydrolyase activity, it can be argued that a likely underlying cause is the mutation-imposed conformational changes given that A219E induced drastic alteration of secondary structures of MtMazG upon Mg^{2+} binding (Fig. 2C). Surprisingly, however, Mg^{2+} at high concentration, while inducing profound alteration in secondary structures, was able to increase the activity of MtMazG[A219E], albeit to a limited extent (Fig. 2B). The mechanistic basis for this partial activation of the MtMazG[A219E] hydrolytic activity by high levels of Mg^{2+} remains to be explored.

Based on the findings that MsMazG and MtMazG have similar enzymatic properties (Table 1), and on the conserved function between these two enzymes in maintaining cell viability under oxidative stress (Fig. 3C), it is likely that MtMazG and MsMazG share similar physiological role, at least to some extent. Apart from this study uncovering a role for MtMazG in oxidative stress response, little is known about the physiological functions of this enzyme. A previous genetic screening study found that the H37Rv *mazG* mutant was attenuated in the mouse infection model (15), implying that *mazG* is a potential virulence factor in *M. tuberculosis*. Rengarajan *et al.* (40) reported that the transcription of H37Rv *mazG* was up-regulated 2.7 times after infection in INF- γ activated macrophage cells. To survive inside the macrophages, *M. tuberculosis* has acquired abilities to withstand the bactericidal host defenses, such as oxidative and nitrosative stress, starvation, hypoxia and acidification (41, 42). It was suggested that to a certain extent, the loss of virulence of the avirulent strain H37Ra may be related to its survival ability inside the macrophages (43). Our work has shown that the H37Ra-derived A219E mutation diminishes the MazG hydrolase activity (Figs. 1 and 2) as well as its capacity to respond to oxidative stress (Fig. 3). Based on these findings, we speculate that H37Ra may lose its virulence partly due to the A219E mutation-caused reduction of MazG hydrolase activity and viability under oxidative stress within the macrophage environment. If validated, this line of research would elucidate MazG as a potentially critical factor that contributes to the virulence of *M. tuberculosis*.

Acknowledgments—We thank Prof. Zhen-Qiang Pan at Mount Sinai School of Medicine, Petros Karakousis at Johns Hopkins University School of Medicine, and Benfang Lei at Montana State University for discussions and critical comments on the manuscript.

REFERENCES

1. Streeken, W., JR, and Gardner, L. U. (1946) *Am. Rev. Tuberc.* **54**, 62–66
2. Zheng, H., Lu, L., Wang, B., Pu, S., Zhang, X., Zhu, G., Shi, W., Zhang, L., Wang, H., Wang, S., Zhao, G., and Zhang, Y. (2008) *PLoS One* **3**, e2375

3. Brosch, R., Philipp, W. J., Stavropoulos, E., Colston, M. J., Cole, S. T., and Gordon, S. V. (1999) *Infect Immun* **67**, 5768–5774
4. Gao, Q., Kripke, K., Arinc, Z., Voskuil, M., and Small, P. (2004) *Tuberculosis* **84**, 188–196
5. He, X. Y., Zhuang, Y. H., Zhang, X. G., and Li, G. L. (2003) *Microbes Infect* **5**, 851–856
6. Lari, N., Rindi, L., Lami, C., and Garzelli, C. (1999) *Microb Pathog* **26**, 281–286
7. Mostowy, S., Cleto, C., Sherman, D. R., and Behr, M. A. (2004) *Tuberculosis* **84**, 197–204
8. Gross, M., Marianovsky, I., and Glaser, G. (2006) *Mol. Microbiol.* **59**, 590–601
9. Galperin, M. Y., Moroz, O. V., Wilson, K. S., and Murzin, A. G. (2006) *Mol. Microbiol.* **59**, 5–19
10. Moroz, O. V., Murzin, A. G., Makarova, K. S., Koonin, E. V., Wilson, K. S., and Galperin, M. Y. (2005) *J. Mol. Biol.* **347**, 243–255
11. Lee, S., Kim, M. H., Kang, B. S., Kim, J. S., Kim, G. H., Kim, Y. G., and Kim, K. J. (2008) *J. Biol. Chem.* **283**, 15232–15240
12. Aizenman, E., Engelberg-Kulka, H., and Glaser, G. (1996) *Proc. Natl. Acad. Sci. U.S.A.* **93**, 6059–6063
13. Zhang, Y., Zhang, J., Hoeflich, K. P., Ikura, M., Qing, G., and Inouye, M. (2003) *Mol. Cell* **12**, 913–923
14. Engelberg-Kulka, H., Hazan, R., and Amitai, S. (2005) *J. Cell Sci.* **118**, 4327–4332
15. Sasseti, C. M., and Rubin, E. J. (2003) *Proc. Natl. Acad. Sci. U.S.A.* **100**, 12989–12994
16. Walker, J. M. (1994) *Methods Mol. Biol.* **32**, 5–8
17. Payandeh, J., Fujihashi, M., Gillon, W., and Pai, E. F. (2006) *J. Biol. Chem.* **281**, 6070–6078
18. Bardarov, S., Bardarov Jr., S., Jr., Pavelka Jr., M. S., Jr., Sambandamurthy, V., Larsen, M., Tufariello, J., Chan, J., Hatfull, G., and Jacobs Jr., W. R., Jr. (2002) *Microbiology* **148**, 3007–3017
19. Sambrook, J., Fritsch, E. F., and Maniatis, T. (1989) *Molecular Cloning: A Laboratory Manual*, 2nd Ed., Cold Spring Harbor Laboratory, Cold Spring Harbor, NY
20. Schnappinger, D., Ehrh, S., Voskuil, M. I., Liu, Y., Mangan, J. A., Monahan, I. M., Dolganov, G., Efron, B., Butcher, P. D., Nathan, C., and Schoolnik, G. K. (2003) *J. Exp. Med.* **198**, 693–704
21. Manganelli, R., Dubnau, E., Tyagi, S., Kramer, F. R., and Smith, I. (1999) *Mol. Microbiol.* **31**, 715–724
22. Robinson, A., Guilfoyle, A. P., Harrop, S. J., Boucher, Y., Stokes, H. W., Curmi, P. M., and Mabbitt, B. C. (2007) *Mol. Microbiol.* **66**, 610–621
23. Zhang, J., and Inouye, M. (2002) *J. Bacteriol.* **184**, 5323–5329
24. Kouzminova, E. A., and Kuzminov, A. (2004) *Mol. Microbiol.* **51**, 1279–1295
25. Zhang, J., Zhang, Y., and Inouye, M. (2003) *J. Biol. Chem.* **278**, 21408–21414
26. Pursell, Z. F., McDonald, J. T., Mathews, C. K., and Kunkel, T. A. (2008) *Nucleic Acids Res.* **36**, 2174–2181
27. Tassotto, M. L., and Mathews, C. K. (2002) *J. Biol. Chem.* **277**, 15807–15812
28. Sekiguchi, M., and Tsuzuki, T. (2002) *Oncogene* **21**, 8895–8904
29. Wu, Q. L., Kong, D., Lam, K., and Husson, R. N. (1997) *J. Bacteriol.* **179**, 2922–2929
30. Sureka, K., Dey, S., Datta, P., Singh, A. K., Dasgupta, A., Rodrigue, S., Basu, J., and Kundu, M. (2007) *Mol. Microbiol.* **65**, 261–276
31. Hu, Y., Kendall, S., Stoker, N. G., and Coates, A. R. (2004) *FEMS Microbiol. Lett.* **237**, 415–423
32. Primm, T. P., Andersen, S. J., Mizrahi, V., Avarbock, D., Rubin, H., and Barry, C. E., 3rd. (2000) *J. Bacteriol.* **182**, 4889–4898
33. Fernandes, N. D., Wu, Q. L., Kong, D., Puyang, X., Garg, S., and Husson, R. N. (1999) *J. Bacteriol.* **181**, 4266–4274
34. Braeken, K., Moris, M., Daniels, R., Vanderleyden, J., and Michiels, J. (2006) *Trends Microbiol.* **14**, 45–54
35. Wu, B., Liu, Y., Zhao, Q., Liao, S., Zhang, J., Bartlam, M., Chen, W., and Rao, Z. (2007) *J. Mol. Biol.* **367**, 1405–1412
36. Maki, H., and Sekiguchi, M. (1992) *Nature* **355**, 273–275
37. Slupphaug, G., Kavli, B., and Krokan, H. E. (2003) *Mutat Res.* **531**, 231–251
38. Dahl, J. L., Kraus, C. N., Boshoff, H. I., Doan, B., Foley, K., Avarbock, D., Kaplan, G., Mizrahi, V., Rubin, H., and Barry, C. E., 3rd. (2003) *Proc. Natl. Acad. Sci. U.S.A.* **100**, 10026–10031
39. Stallings, C. L., Stephanou, N. C., Chu, L., Hochschild, A., Nickels, B. E., and Glickman, M. S. (2009) *Cell* **138**, 146–159
40. Rengarajan, J., Bloom, B. R., and Rubin, E. J. (2005) *Proc. Natl. Acad. Sci. U.S.A.* **102**, 8327–8332
41. Ehrh, S., and Schnappinger, D. (2009) *Cell Microbiol.* **11**, 1170–1178
42. Chan, J., Xing, Y., Magliozzo, R. S., and Bloom, B. R. (1992) *J. Exp. Med.* **175**, 1111–1122
43. Mackaness, G. B., Smith, N., and Wells, A. Q. (1954) *Am. Rev. Tuberc.* **69**, 479–494